Fast Synthesis of High-Performance Graphene Films by Hydrogen-Free Rapid Thermal Chemical Vapor Deposition

Jaechul Ryu,[†,‡,▽] Youngsoo Kim,[⊥,▽] Dongkwan Won,[†] Nayoung Kim,[†] Jin Sung Park,[†] Eun-Kyu Lee,[†] Donyub Cho,[†] Sung-Pyo Cho,[§] Sang Jin Kim,[§] Gyeong Hee Ryu,[#] Hae-A-Seul Shin,[∥] Zonghoon Lee,[#] Byung Hee Hong,[‡,§,△,*] and Seungmin Cho[†,*]

[†]Micro Device & Machinery Solution Division, Samsung Techwin R&D Center, Seongnam-si, Gyeonggi-do, 463-400, Republic of Korea, [‡]SKKU Advanced Institute of Nanotechnology (SAINT) and Center for Human Interface Nano Technology (HINT), [§]Department of Chemistry, [⊥]Department of Physics & Astronomy, and [∥]Department of Materials Science & Engineering, Seoul National University, Seoul 151-747, Republic of Korea, [#]School of Mechanical and Advanced Materials Engineering, Ulsan National Institute of Science and Technology (UNIST), Ulsan 689-798, Republic of Korea, and [△]Graphene Square Inc., Inter-University Semiconductor Research Center, Seoul 151-747, Republic of Korea. [▽]J. Ryu and Y. Kim contributed equally.

ABSTRACT

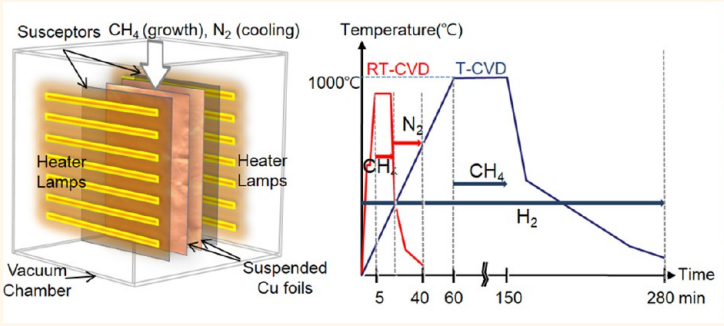

The practical use of graphene in consumer electronics has not been demonstrated since the size, uniformity, and reliability problems are yet to be solved to satisfy industrial standards. Here we report mass-produced graphene films synthesized by hydrogen-free rapid thermal chemical vapor deposition (RT-CVD), roll-to-roll etching, and transfer methods, which enabled faster and larger production of homogeneous graphene films over 400 × 300 mm^2 area with a sheet resistance of 249 ± 17 Ω/sq without additional doping. The properties of RT-CVD graphene have been carefully characterized by high-resolution transmission electron microscopy, Raman spectroscopy, chemical grain boundary analysis, and various electrical device measurements, showing excellent uniformity and stability. In particular, we found no significant correlation between graphene domain sizes and electrical conductivity, unlike previous theoretical expectations for nanoscale graphene domains. Finally, the actual application of the RT-CVD films to capacitive multitouch devices installed in the most sophisticated mobile phone was demonstrated.

KEYWORDS: graphene · transparent · flexible · foldable · touch screen · chemical vapor deposition

Graphene and related materials have been intensively studied for the past few years due to their fascinating electrical,[1] mechanical,[2] and chemical[3] properties. There have been many efforts to utilize these fascinating properties of graphene for macroscopic applications such as transparent conducting films useful for flexible electronics.[4] The implementation of graphene requires a production worthy process, and it has been successfully demonstrated that a thermal chemical vapor deposition (T-CVD) process is capable of growing high-quality graphene on Cu substrates.[5−7] This approach was found to be easily scalable up to meter sizes by employing roll-to-roll (R2R) methods.[7] Even though the scalable production of graphene by R2R etching and transfer methods has been suggested previously,[7] the typical T-CVD process that takes a few hours from heating and synthesis to cooling (Figure 1b) practically limits the throughput of graphene production. In addition, the synthesis

* Address correspondence to byunghee@snu.ac.kr (B. H. Hong); seungmin.cho@samsung.com (S. Cho).

Received for review November 5, 2013 and accepted December 22, 2013.

Published online December 23, 2013
10.1021/nn405754d

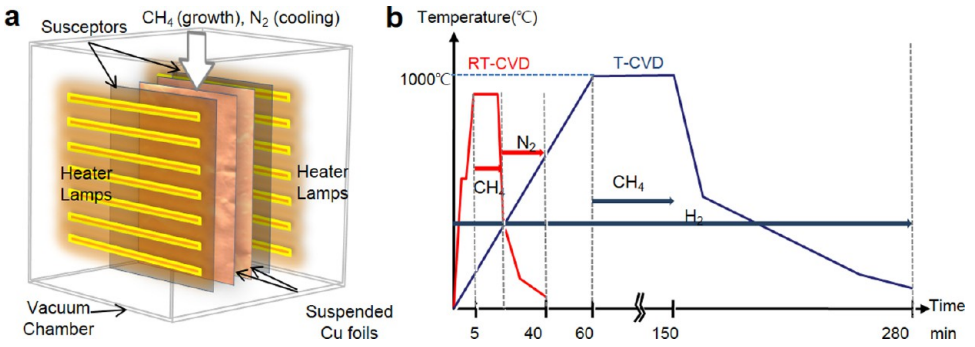

Figure 1. (a) Schematic illustration of RT-CVD synthesis setup. The graphite susceptors between heater lamps and Cu foils convert near-IR lights into thermal radiation. CH_4 and N_2 gases are used for growth and cooling processes, respectively. The Cu foils are suspended vertically during the growth. (b) Graphene growth conditions of RT-CVD compared with T-CVD.

temperature, as high as ~1000 °C, often results in contamination by evaporated Cu, leading to the formation of defective graphene structures (Figure S7). The safety issue associated with the use of hydrogen gas also needs to be solved for mass production, and the hydrogen-free process was first reported in the growth of graphene on Ni by plasma-enhanced CVD (PE-CVD).[8] On the other hand, rapid thermal annealing was suggested as an efficient heating method to synthesize high-quality graphene at lower temperature.[9] However, the hydrogen-free synthesis of large-area graphene on Cu foils with mass-production scale, quality, and uniformity has not been successfully demonstrated.

Recently, efforts have been devoted to perfect the CVD synthesis at lower temperature not only by adopting more efficient heating methods[10,11] but by alloying,[12] annealing,[7] or polishing catalytic substrates,[13] leading to larger single-crystalline domains and less structural defects such as grain boundaries[14] and ripples.[15] Nevertheless, the previously proposed high-throughput graphene synthesis methods based on Joule-heating[9] and microwave plasma[10] are found to yield either multilayered or defective graphene films whose sheet resistances are not suitable for touch screen applications.[4] In addition, the strong chemical doping to enhance conductivity is not desirable because it does not persist long enough for practical applications without proper encapsulation.[16] New equipment based on RT-CVD has been designed and manufactured for the following purposes: (i) to maintain the high quality of graphene at lower synthesis temperature without using hydrogen gas; (ii) to minimize growth time for high-throughput production; and (iii) to achieve size, uniformity, reliability, durability, and flexibility needed for industrial applications.

RESULT AND DISCUSSION

Figure 1 shows a schematic representation of the RT-CVD synthesis setup. First, Cu foils (35 μm thick, 99.85% purity) were vertically loaded to prevent deformation caused by thermal expansion and gravity, and then, the whole chamber was vacuumed below 2 mTorr

TABLE 1. Comparisons of T-CVD-Grown Graphene and RT-CVD-Grown Graphene Sample

	graphene growth rate (cm^2/h)	synthesis temperature (°C)	use of H_2 gas	carrier gas	mobility (cm^2/(V s)) at 297 K
T-CVD[18]	~200	1000	yes	Ar	~5100
RT-CVD	~1400	970	no	N_2	~5200

for a few minutes. The heating unit is composed of 24 halogen lamps radiating light ranging from visible to infrared (IR) wavelengths, which is advantageous in terms of growth area per time compared to conventional thermal heating methods utilizing open wire-coil sources (Figure 1a and Table 1). However, the radiation close to visible wavelength is mostly reflected by the Cu surface, and a temperature as high as 1000 °C cannot be easily reached due to the energy loss. Thus, we adopted a graphite susceptor that efficiently transforms near-infrared light to thermal radiation.[9] It is also noteworthy that the high thermal conductivity of graphite additionally enhances the uniformity of heat distribution on the Cu surface. The reaction temperature was carefully monitored at five different positions using embedded thermocouples, which has been optimized to be ~970 °C for the highest quality graphene synthesis. This temperature is slightly lower than the T-CVD temperature (~1000 °C), but it is low enough to prevent contamination by Cu evaporation. In the T-CVD system, the high energy needed for graphene growth is delivered by radiant heat from hot coils outside the quartz chamber to the Cu substrates inside. In this case, the temperature on the Cu foil surface is always lower than the hot coils, so the chamber needs to be slightly overheated. However, in the RT-CVD system, the halogen lamps inside the chamber deliver shorter-wavelength radiation to a graphite susceptor that converts the radiation into thermal energy. Therefore, the highest temperature region is very close to the Cu surface, and the growth of graphene can occur more efficiently at lower heater temperature. In addition, the heating time of hot coils is usually an hour long because the

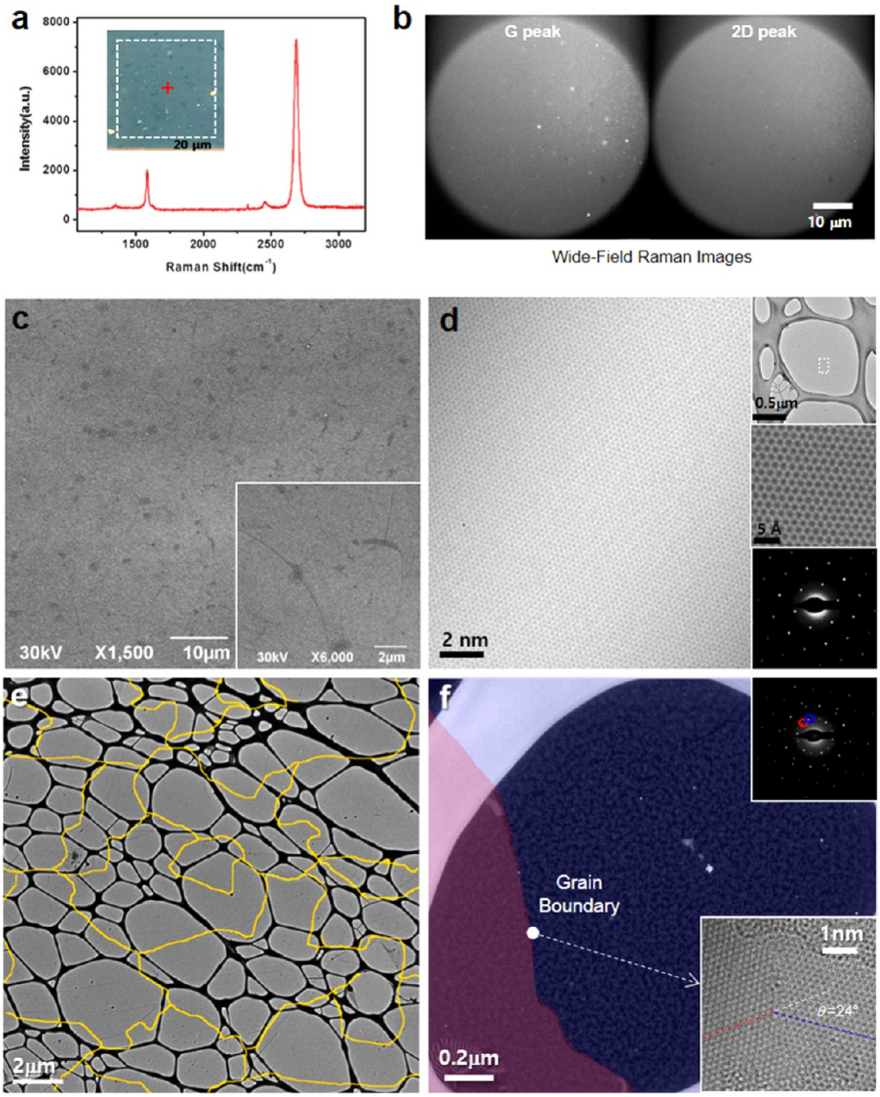

Figure 2. Spectroscopic analyses of RT-CVD graphene films. (a) Representative single-point Raman spectrum indicating the growth of high-quality graphene films. The inset shows an optical microscope image of RT-CVD graphene transferred by TRT methods on a SiO_2 substrate. (b) Wide-field (WF) Raman images filtered at G and 2D peak ranges, showing the uniformity of graphene films in real time. (c) SEM images of graphene on SiO_2 showing ripples and adlayers, but no cracks. (d) HR-TEM results showing the atomic lattice structures of RT-CVD graphene. The graphene samples were prepared with holey carbon grids (upper inset). The aberration-corrected scanning TEM image provides an atom-by-atom analysis of graphene (mid inset). The diffraction pattern indicates the corresponding graphene is a highly crystalline monolayer (lower inset). (e) Graphene domain distribution investigated by selected area diffraction patterns (SADP) and TEM imaging. (f) Graphene boundaries of RT-CVD graphene characterized by dark-field TEM and aberration-corrected HR-TEM images. The left and right parts of the grain boundary are imaged with an aperture at the red and blue circled spots of the diffraction pattern (upper inset). The atomic image shows that two graphene domains are smoothly connected with an angle of 36° (lower inset). See also Supporting Figure S2 for more dark-field TEM analyses.

whole chamber needs to be heated together, but the RT-CVD needs only a few minutes from room temperature to 970 °C because only the susceptor and Cu surface are intensively heated. For the same reason, cooling is also faster for RT-CVD than for T-CVD. This is very critical for the simple and cost-effective design of the R2R synthesis system. For example, cheaper and more easily processible stainless steel chambers can be used for RT-CVD, but T-CVD usually requires more expensive and hard-to-shape quartz or ceramic chambers.

After the temperature is stabilized, methane (CH_4, 99.999%) gas was flowed with a rate of 50 sccm at 550 mTorr. After 5 mins, the chamber was cooled to 600 °C with a rate of 1.5 °C/s with flowing 50 sccm CH_4 at 550 mTorr. At 600 °C, nitrogen (N_2) gas (~5000 sccm) was flushed into the chamber so that the foils are rapidly cooled to room temperature. Thus, the whole RT-CVD synthesis process is ~40 mins long and hydrogen gas free, which is advantageous for higher production throughput and for better safety, respectively (Figure 1b). After the growth, the graphene film on the Cu foil was attached to a thermal release tape (TRT, Jinsung Chemical Co.) using a laminator with accurately controlled pressure and temperature.[3]

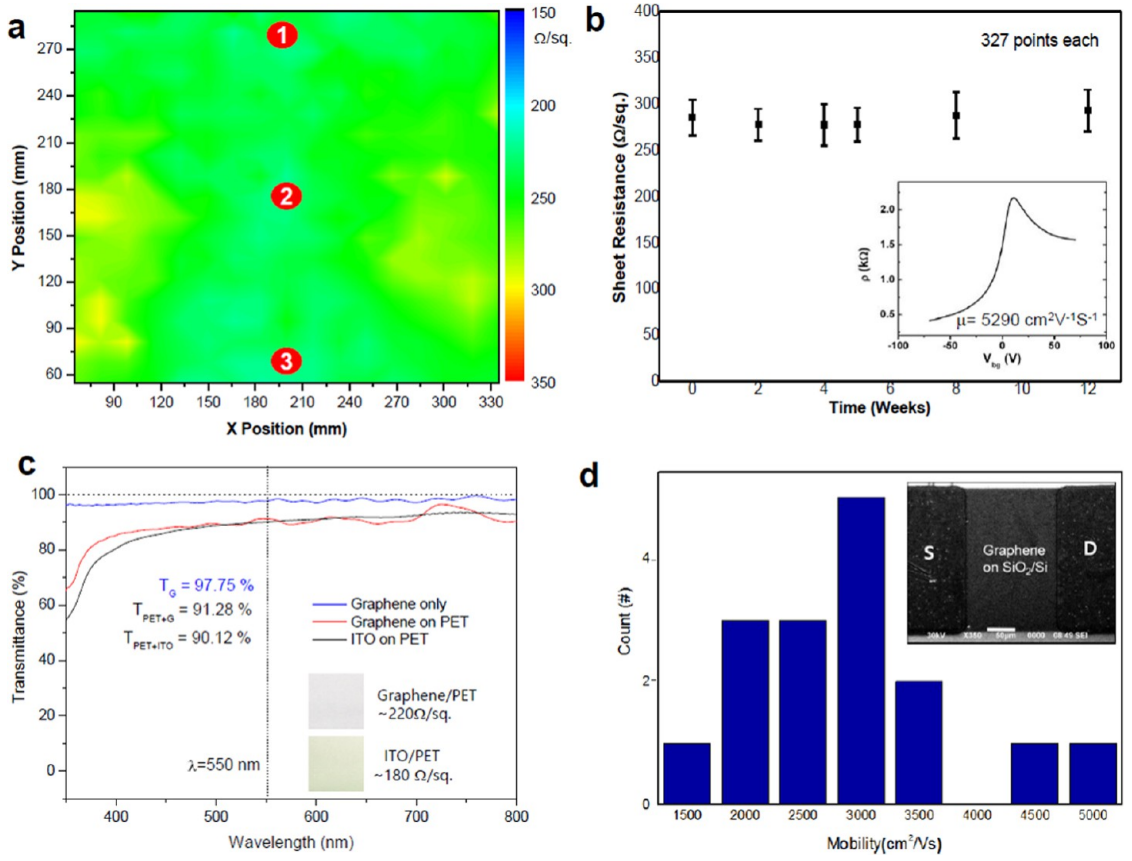

Figure 3. Electrical and optical analyses of RT-CVD graphene films. (a) Sheet resistance mapping of graphene film on PET showing sheet resistance distribution of 249 ± 17 Ω/sq. (b) Durability analysis of RT-CVD graphene films for 12 weeks, showing less than 10% deviation from the initial value. The inset shows that the charge carrier mobility measured in a graphene FET is as high as 5290 $cm^2\ V^{-1}s^{-1}$. (c) UV−Vis transmittance spectra of the graphene film on PET. The 2.25% absorption at λ = 550 nm indicates that the graphene films are mostly single layers. (d) Charge carrier mobility distribution measured in RT-CVD graphene FET devices. The inset shows the SEM image of the FET device.

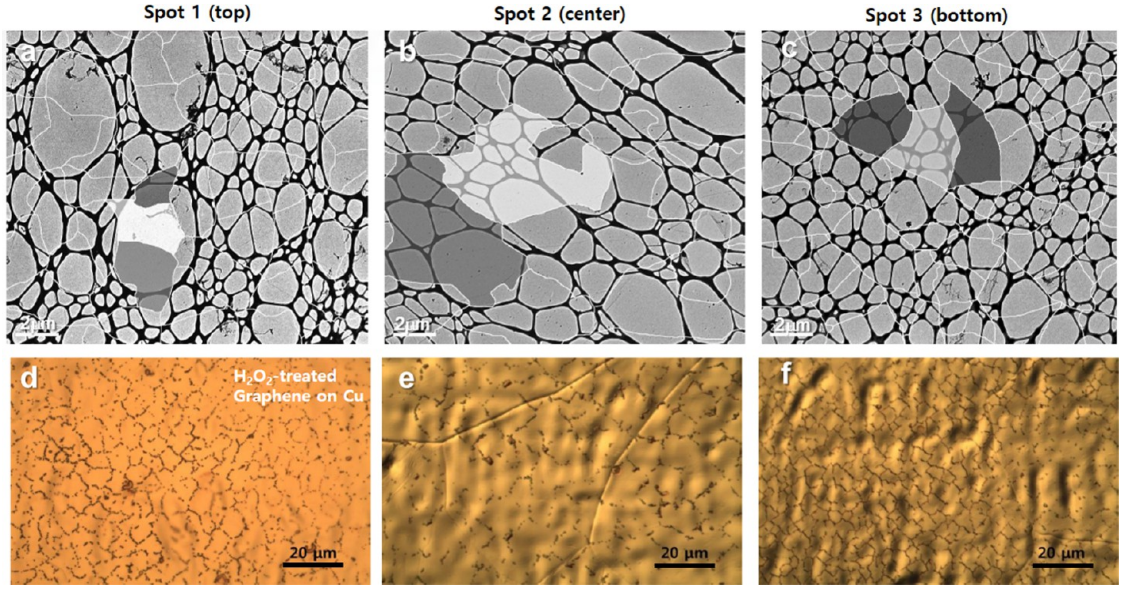

Figure 4. Grain boundary analyses by TEM and OM. (a−c) Grain boundary mapping of RT-CVD graphene films by TEM corresponding to the sheet resistance of spots 1, 2, and 3 in Figure 3a, respectively. (d−f) Grain boundary mapping of H_2O_2-treated RT-CVD graphene on Cu foils by optical microscopes, corresponding to the red spots 1, 2, and 3 in Figure 3a, respectively. The grain size of graphene in the center region is a few times larger than the edge region, but actually, there is no significant difference in sheet resistance (226, 227, and 230 Ω/sq for spots 1, 2, and 3, respectively).

Figure 5. Photographs of the fabrication processes of graphene-based capacitive touch-screen devices. (a) Graphene on a Cu foil after RT-CVD growth. (b) TRT layer laminated on top of the graphene/Cu film at room temperature. (c) Graphene on a PET film after etching Cu and detaching TRT by hot laminating. (d) Patterned graphene/PET film by photolithography and O_2 plasma etching. (e) Screen-printed Ag electrodes on top of the patterned graphene electrodes. (f) Complete set of assembled layers including upper and lower graphene electrodes with an OCA layer in between. (g) Photograph of the graphene touch screen installed in a mobile phone (left) in comparison with an ITO-based touch screen phone (right).

Then, hydrogen peroxide and sulfuric acid based etching solution[17] was spayed to remove the Cu on the other side of the TRT as it passed through the R2R etching system,[7] where the backside graphene was removed together with dissolved Cu. After fully etching the Cu foil, the graphene attached to the TRT was rinsed with deionized (DI) water. Subsequently, the graphene film on TRT was inserted into the R2R laminator together with a target substrate. In this step, we used 100 μm thick polyethylene terephthalate (PET) substrates whose glass transition temperature (T_g) is ~120 °C. As passing through the laminator at 110 °C with a speed of 0.5 m/min and ~0.4 MPa pressure between rollers, the graphene films were successfully transferred onto the target substrate as TRT loses its adhesive force at the elevated temperature.[3] The R2R-transferred graphene tends to follow the surface morphology of the substrates, which maximizes the van der Waals contact area between graphene and PET. Therefore, no adhesive layer was needed between graphene and PET.[18] The transferred graphene film was patterned by screen-masked and O_2 plasma etching for device fabrication.[19] Therefore, no photoresist coating and lift-off processes were used, which is advantageous for

cost-effective fabrication of graphene-based electronic devices. The whole graphene synthesis and film fabrication processes were automated, as shown in Figure S1.

The properties of graphene films produced by RT-CVD were carefully characterized by various spectroscopic methods including Raman spectroscopy and high-resolution transmission electron microscopy (HR-TEM). Raman spectra (Figure 2a)[20] and wide-field Raman (WF-Raman)[21] images (Figure 3b) show that the graphene films are dominantly monolayers with more than 95% coverage. In particular, the WF-Raman method is useful to monitor the thickness and the quality of graphene films in real time,[21] which is an essential step to ensure production yields. A comparison between WF-Raman and micro-Raman mapping is shown in Figure S5. Scanning electron microscope (SEM) images, HR-TEM images[12,22] (JEOL JEM-ARM200F, JEM-3010 and FEI Titan Cube G2), and diffraction patterns analysis show that the atomic structures of RT-CVD graphene are highly crystalline, and the sizes of graphene domains are 3−12 μm (Figure 2c−f and Figure S1).

The representative sheet resistance distribution measured over a 400 × 300 mm^2 graphene/PET film is 249 ± 17 Ω/sq, which qualifies for an industrial standard for transparent electrodes requiring 10% deviation or less (Figure 3a; see also Figure S6a for full area mapping). To check the reproducibility of the RT-CVD method, we measured 10 different graphene samples sequentially grown at the same growth condition. The sheet resistance variation is measured to be only 232 ± 36 Ω/sq (Figure S6), which indicates that the RT-CVD method is reliable enough for the repetitive growth of large-area graphene. It should be noted that such uniformity and reproducibility was hardly achievable by T-CVD methods.[3] Moreover, the sheet resistance persists for more than 12 weeks at ambient conditions (Figure 3b). We supposed that the remnants of the strongly p-doping etchants are captured between graphene and the substrate after TRT transfer, which considerably enhances the conductivity of graphene films with extraordinary stability. Indeed, the field-effect transistor (FET) characteristic (Figure 3b, inset) indicates that as-grown RT-CVD graphene is unusually p-doped and the mobility is as high as 5290 cm^2 V^{-1} s^{-1} at room temperature (Figure 3d). UV−vis spectroscopic analysis shows that the graphene/PET films are transparent for all visible wavelengths, while indium tin oxides (ITO), the most popular transparent conducting materials, are less transparent in short visible wavelength ranges, which appears to be slightly yellowish (Figure 3c).[23]

It has been reported that the grain size of graphene is an important factor that determines its conductivity based on the theoretical modeling.[24] Thus, we tried to check the correlation between the grain size and the sheet resistance of the RT-CVD graphene. The graphene samples with different grain sizes were obtained from the three different regions corresponding to spots 1, 2, and 3 in Figure 3a. The grain size distribution of graphene on Cu foils can be optically characterized after H_2O_2 treatment as shown in Figure 4d,e,[25] which matches well with the grain boundary mapping by TEM diffraction (Figure 4a−c). The grain sizes at the center region (spot 1) are found to be a few times larger than the edge region (spots 1 and 3), which is probably due to the inhomogeneous temperature gradient. However, the sheet resistances measured from the three spots are not significantly different, although their grain sizes are clearly different, implying that the grain size factor becomes less dominant as the scale increases from nanometer to micrometer scale, and other factors such as doping strength, defect density, and phonon scattering by nanoripples[15] are more important for conductivity.

Finally, we demonstrated the actual application of the RT-CVD graphene for capacitive multitouch screens that are fully functional in the most sophisticated mobile phone (Figure 5g and Supporting Movie S1). The whole fabrication was processed with 400 × 300 mm^2 RT-CVD graphene films from roll-to-roll etching, O_2 plasma patterning, Ag electrode printing, to final assembly (Figure 5a−f; see Supporting Figure S3 for fabrication details). The resulting multitouch device worked perfectly with the most sophisticated mobile phone (Movies S1 and S2), which is believed to be the first demonstration of graphene application to actual consumer electronics devices.

CONCLUSION

In conclusion, we have demonstrated RT-CVD growth, etching, and transfer systems that are mass-production compatible. The RT-CVD is advantageous not only because of the fast heating and cooling processes but because of hydrogen-free and lower temperature growth conditions. The outstanding properties of the RT-CVD graphene were confirmed by Raman spectroscopy, HR-TEM, and various electrical characterizations. Especially, the correlation between graphene grain size and the conductivity is found to be no more effective in the case where the grain is more than a few micrometers large. We believe the RT-CVD method would be one of the best ways to mass-produce the high-quality graphene films satisfying the industrial standards needed for transparent conductors, which will facilitate various graphene-based applications[26−30] as well as bring the advent of graphene-based consumer electronic devices forward.

EXPERIMENTAL SECTION

Sample Preparation. We used H_2O_2 and H_2SO_4 (5:5) as Cu etchant, rinsed in DI water. The typical etching time for 35 μm thick Cu foil is ~20 min. Graphene samples were transferred by the TRT method on a SiO_2/Si substrate for Raman and electrical characterization after washing with DI water several times.[6]

The graphene samples for FET measurements were annealed in an Ar/H_2 gas environment at 300 °C. The full fabrication processes of the graphene FET device are illustrated in Figure S4.

Characterization. Micro-Raman spectra were obtained using a 1 mW 514 nm Ar laser with a spot size of 2 μm (Renishaw inVia Raman Microscope). A homemade WF-Raman microscope equipped with a 532 nm excitation laser was used to characterize RT-CVD graphene. The measurements of graphene field effect transistors were performed by using the three-terminal mode of an Agilent 2602 system applying 10 mV source−drain voltage. The sheet resistance mapping of the large-area RT-CVD graphene (400 × 300 mm^2) was carried out by a fully automated measurement setup (Dasol ENG RS8-1G) based on the van der Pauw method considering

$$R_s = \frac{\pi}{\ln 2}\frac{V}{I}$$

where R_s is sheet resistance, V is applied voltage, and I is current. The operation of the graphene-based touch screen installed in a commercial smart phone is demonstrated in Movies S1 and S2.

Conflict of Interest: The authors declare no competing financial interest.

Acknowledgment. This work was supported by the Global Research Lab (GRL) Program (2013-056425), the Global Frontier Research Program (2011-0031629), and the Basic Science Research Program (2012M3A7B4049807, 2011K000615, 2011-0017587, 2009-0083540) through the National Research Foundation of Korea (NRF) funded by the Ministry of Science, ICT and Future Planning and by Industrial Core Technology Development Program (10033309) and Technology Innovation Program (10044410) of the Ministry of Trade, Industry and Energy.

Supporting Information Available: Additional information and figures. This material is available free of charge *via* the Internet at http://pubs.acs.org.

REFERENCES AND NOTES

1. Geim, A. K.; Novoselov, K. S. The Rise of Graphene. *Nat. Mater.* **2007**, *6*, 183–191.
2. Lee, C.; Wei, X.; Kysar, J. W.; Hone, J. Measurement of the Elastic Properties and Intrinsic Strength of Monolayer Graphene. *Science* **2008**, *321*, 385–388.
3. Loh, K. P.; Bao, Q.; Eda, G.; Chhowalla, M. Graphene Oxide as a Chemically Tunable Platform for Optical Applications. *Nat. Chem.* **2010**, *2*, 1015–1024.
4. Bae, S.; Kim, S. J.; Shin, D.; Ahn, J.-H.; Hong, B. H. Towards Industrial Applications of Graphene Electrodes. *Phys. Scr.* **2012**, *T146*, 014024.
5. Kim, K. S.; Zhao, Y.; Jang, H.; Lee, S. Y.; Kim, J. M.; Kim, K. S.; Ahn, J.-H.; Kim, P.; Choi, J.-Y.; Hong, B. H. Large-Scale Pattern Growth of Graphene Films for Stretchable Transparent Electrodes. *Nature* **2009**, *457*, 706–710.
6. Li, X.; Cai, W.; An, J.; Kim, S.; Nah, J.; Yang, D.; Piner, R.; Velamakanni, A.; Jung, I.; Tutuc, E.; *et al.* Large-Area Synthesis of High-Quality and Uniform Graphene Films on Copper Foils. *Science* **2009**, *324*, 1312–1314.
7. Bae, S.; Kim, H.; Lee, Y.; Xu, X.; Park, J.-S.; Zheng, Y.; Balakrishnan, J.; Lei, T.; Ri Kim, H.; Song, Y. I.; *et al.* Roll-to-Roll Production of 30-Inch Graphene Films for Transparent Electrodes. *Nat. Nanotechnol.* **2010**, *5*, 574–578.
8. Peng, K.-J.; Wu, C.-L.; Lin, Y.-H.; Liu, Y.-J.; Tsai, D.-P.; Pai, Y.-H.; Lin, G.-R. Hydrogen-Free PECVD Growth of Few-Layer Graphene on an Ultra-Thin Nickel Film at the Threshold Dissolution Temperature. *J. Mater. Chem. C* **2013**, *1*, 3862–3870.
9. Kim, W.; Riikonen, J.; Arpiainen, S.; Svensk, O.; Li, C.; Lipsanen, H. Growth of CVD Graphene on Copper by Rapid Thermal Processing. *MRS Proc.* **2012**, *1451*, 27–32.
10. Yamada, T.; Ishihara, M.; Kim, J.; Hasegawa, M.; Iijima, S. A Roll-to-Roll Microwave Plasma Chemical Vapor Deposition Process for the Production of 294 mm Width Graphene Films at Low Temperature. *Carbon* **2012**, *50*, 2615–2619.
11. Kobayashi, T.; Bando, M.; Kimura, N.; Shimizu, K.; Kadono, K.; Umezu, N.; Miyahara, K.; Hayazaki, S.; Nagai, S.; Mizuguchi, Y.; *et al.* Production of a 100-m-Long High-Quality Graphene Transparent Conductive Film by Roll-to-Roll Chemical Vapor Deposition and Transfer Process. *Appl. Phys. Lett.* **2013**, *102*, 023112–023112−4.
12. Edwards, R. S.; Coleman, K. S. Graphene Film Growth on Polycrystalline Metals. *Acc. Chem. Res.* **2012**, *46*, 23–30.
13. Luo, Z.; Lu, Y.; Singer, D. W.; Berck, M. E.; Somers, L. A.; Goldsmith, B. R.; Johnson, A. T. C. Effect of Substrate Roughness and Feedstock Concentration on Growth of Wafer-Scale Graphene at Atmospheric Pressure. *Chem. Mater.* **2011**, *23*, 1441–1447.
14. Huang, P. Y.; Ruiz-Vargas, C. S.; van der Zande, A. M.; Whitney, W. S.; Levendorf, M. P.; Kevek, J. W.; Garg, S.; Alden, J. S.; Hustedt, C. J.; Zhu, Y.; *et al.* Grains and Grain Boundaries in Single-Layer Graphene Atomic Patchwork Quilts. *Nature* **2011**, *469*, 389–392.
15. Ni, G.-X.; Zheng, Y.; Bae, S.; Kim, H. R.; Pachoud, A.; Kim, Y. S.; Tan, C.-L.; Im, D.; Ahn, J.-H.; Hong, B. H.; *et al.* Quasi-Periodic Nanoripples in Graphene Grown by Chemical Vapor Deposition and Its Impact on Charge Transport. *ACS Nano* **2012**, *6*, 1158–1164.
16. Yan, C.; Kim, K.-S.; Lee, S.-K.; Bae, S.-H.; Hong, B. H.; Kim, J.-H.; Lee, H.-J.; Ahn, J.-H. Mechanical and Environmental Stability of Polymer Thin-Film-Coated Graphene. *ACS Nano* **2011**, *6*, 2096–2103.
17. Schellinger, R., Jr.Composition and Process for Printed Circuit Etching Using a Sulfuric Acid Solution Containing Hydrogen Peroxide. US Patent4401509, 1983.
18. Kang, J.; Shin, D.; Bae, S.; Hong, B. H. Graphene Transfer: Key for Applications. *Nanoscale* **2012**, *4*, 5527–5537.
19. Lee, Y.; Bae, S.; Jang, H.; Jang, S.; Zhu, S.-E.; Sim, S. H.; Song, Y. I.; Hong, B. H.; Ahn, J.-H. Wafer-Scale Synthesis and Transfer of Graphene Films. *Nano Lett.* **2010**, *10*, 490–493.
20. Ferrari, A. C.; Meyer, J. C.; Scardaci, V.; Casiraghi, C.; Lazzeri, M.; Mauri, F.; Piscanec, S.; Jiang, D.; Novoselov, K. S.; Roth, S.; *et al.* Raman Spectrum of Graphene and Graphene Layers. *Phy. Rev. Lett.* **2006**, *97*, 187401.
21. Havener, R. W.; Ju, S.-Y.; Brown, L.; Wang, Z.; Wojcik, M.; Ruiz-Vargas, C. S.; Park, J. High-Throughput Graphene Imaging on Arbitrary Substrates with Widefield Raman Spectroscopy. *ACS Nano* **2011**, *6*, 373–380.
22. Kim, K.; Lee, Z.; Regan, W.; Kisielowski, C.; Crommie, M. F.; Zettl, A. Grain Boundary Mapping in Polycrystalline Graphene. *ACS Nano* **2011**, *5*, 2142–2146.
23. Bonaccorso, F.; Sun, Z.; Hasan, T.; Ferrari, A. C. Graphene Photonics and Optoelectronics. *Nat. Photonics* **2010**, *4*, 611–622.
24. Tuan, D. V.; Kotakoski, J.; Louvet, T.; Ortmann, F.; Meyer, J. C.; Roche, S. Scaling Properties of Charge Transport in Polycrystalline Graphene. *Nano Lett.* **2013**, *13*, 1730–1735.
25. Jia, C.; Jiang, J.; Gan, L.; Guo, X.Direct Optical Characterization of Graphene Growth and Domains on Growth Substrates. *Sci. Rep.* **2012**, *2*.
26. Kang, J.; Kim, H.; Kim, K. S.; Lee, S. K.; Bae, S.; Ahn, J.-H.; Kim, Y. J.; Choi, J. B.; Hong, B. H. High-Performance Graphene-Based Transparent Flexible Heaters. *Nano Lett.* **2011**, *11*, 5154–5158.
27. Ha, J.; Park, S.; Kim, D.; Ryu, J.; Lee, C.; Hong, B. H.; Hong, Y. High-Performance Polymer Light Emitting Diodes with Interface-Engineered Graphene Anodes. *Org. Electron.* **2013**, *14*, 2324–2330.
28. Han, T.-H.; Lee, Y.; Choi, M.-R.; Woo, S.-H.; Bae, S.-H.; Hong, B. H.; Ahn, J.-H.; Lee, T.-W. Extremely Efficient Flexible Organic Light-Emitting Diodes with Modified Graphene Anode. *Nat. Photonics* **2012**, *6*, 105–110.
29. Jo, S. B.; Park, J.; Lee, W. H.; Cho, K.; Hong, B. H. Large-Area Graphene Synthesis and Its Application to Interface-Engineered Field Effect Transistors. *Solid State Commun.* **2012**, *152*, 1350–1358.
30. Jang, J.; Park, J.; Nam, S.; Anthony, J. E.; Kim, Y.; Kim, K. S.; Kim, K. S.; Hong, B. H.; Park, C. E. Self-Organizing Properties of Triethylsilylethynyl-Anthradithiophene on Monolayer Graphene Electrodes in Solution-Processed Transistors. *Nanoscale* **2013**, *5*, 11094–11101.